Contribution from the Department of Chemistry,
Stanford University, Stanford, California 94305

Selenium Substitution in $[Fe_4S_4(SR)_4]^{2-}$: Synthesis and Comparative Properties of $[Fe_4X_4(YC_6H_5)_4]^{2-}$ (X, Y = S, Se) and the Structure of $[(CH_3)_4N]_2[Fe_4Se_4(SC_6H_5)_4]$

M. A. BOBRIK, E. J. LASKOWSKI, RICHARD W. JOHNSON,[1a] W. O. GILLUM, J. M. BERG,
KEITH O. HODGSON,[1b] and R. H. HOLM*

Received July 21, 1977

By a combination of direct synthesis and ligand-exchange reactions the series of tetranuclear dianions $[Fe_4X_4(YPh)_4]^{2-}$ (X, Y = S, Se) has been synthesized. The series consists of $[Fe_4S_4(SPh)_4]^{2-}$, $[Fe_4S_4(SePh)_4]^{2-}$, $[Fe_4Se_4(SPh)_4]^{2-}$, and $[Fe_4Se_4(SePh)_4]^{2-}$, in which sets of four equivalent sulfur and selenium atoms act as terminal and bridging ligands. Properties of series members were compared in order to examine the consequence of S/Se substitution. The cubane-type geometry previously established for $[Fe_4S_4(SPh)_4]^{2-}$ has been confirmed for $[Fe_4Se_4(SPh)_4]^{2-}$ as its Me_4N salt. This compound crystallizes in space group $P2_12_12_1$ of the orthorhombic system with dimensions a = 11.930 (3) Å, b = 24.126 (5) Å, and c = 14.782 (4) Å (Z = 4). The Fe_4Se_4 core is distorted toward D_{2d} symmetry with four short (2.385 (2) Å) and eight long (2.417 (5) Å) Fe–Se distances, giving an average of 2.406 Å; the mean Fe···Fe distance is 2.783 Å. Differences in the core structures of $[Fe_4S_4(SPh)_4]^{2-}$ and $[Fe_4Se_4(SPh)_4]^{2-}$ are small and fully accountable in terms of the larger covalent radius of and the smaller angles generally formed by selenium. Compared to $[Fe_4S_4(SPh)_4]^{2-}$ selenium-containing complexes exhibit red-shifted charge-transfer spectra and small positive shifts of potentials for the couples $[Fe_4X_4(YPh)_4]^{2-/3-}$. EPR spectra of trianions are axial and indicate equivalent ground-state electronic structures for all members of the series. The collective comparative properties of the series confirm selenium as a fully functional substitute for sulfur and support the possibility that selenium could be found in protein 4-Fe centers.

Introduction

The tetranuclear cluster dianions $[Fe_4S_4(SR)_4]^{2-}$ (I) consist

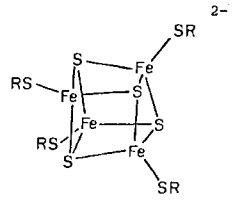

I

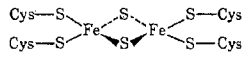

II

of bonding Fe_4 and nonbonding S_4 interpenetrating near-tetrahedral units which form an Fe_4S_4 core of idealized D_{2d} symmetry terminally ligated by thiolate.[2-4] These complexes and the binuclear dianions $[Fe_2S_2(SR)_4]^{2-}$[5] enjoy substantial utility as analogues of the iron–sulfur protein sites I (R = Cys) and II, respectively, in equivalent oxidation levels.[6,7] Certain of our recent investigations of these binuclear and tetranuclear species have been directed toward the fundamental chemical matters of Fe_2S_2/Fe_4S_4 core structural conversion[8] and the effects of terminal ligand variation[9] on cluster properties. Thus far the only nonthiolate ligands which have been shown to bind to both Fe_2S_2 and Fe_4S_4 cores in compounds that have been isolated are halides, which furnish the series $[Fe_2S_2X_4]^{2-}$ and $[Fe_4S_4X_4]^{2-}$ (X = Cl, Br, I).[9] Within these series and in comparison to corresponding thiolate complexes,[2-7] halide substitution effects substantial changes in 2−/3− redox potentials and absorption spectra.[9b,c] Based on results for $[Fe_2S_2Cl_4]^{2-}$ and $[Fe_4S_4Cl_4]^{2-}$, there are no important changes in core dimensions[9a] and magnetic properties[9b] when compared to analogous thiolate derivatives.

In order to examine further the response of the clusters I to changes in bridging and terminal ligands, selenium has been introduced in both binding positions by a combination of direct synthesis[2] and ligand-exchange reactions.[3] By these means the series $[Fe_4X_4(YPh)_4]^{2-}$ (X, Y = S, Se) has been generated. This series may be considered complete in that the complexes $[Fe_4S_4(SPh)_4]^{2-}$,[3,5,10] $[Fe_4S_4(SePh)_4]^{2-}$, $[Fe_4Se_4(SPh)_4]^{2-}$, and $[Fe_4Se_4(SePh)_4]^{2-}$, arising from synthetically feasible "permutations" of four equivalent sulfur and selenium atoms, have all been isolated. This report deals with the synthesis of the series $[Fe_4X_4(YPh)_4]^{2-}$, comparative physical properties of its four members, and the structure of $(Me_4N)_2[Fe_4Se_4(SPh)_4]$. The structure of an isomorphous form of $(Me_4N)_2[Fe_4S_4(SPh)_4]$ has been described earlier.[3]

Selenide has been substituted in the bridging positions of the native protein site II affording Fe_2SSe[11] and Fe_2Se_2[11-13] core units, but no tetranuclear protein sites containing selenide have been described. In addition to providing likely indications of the structural and physicochemical properties of the latter sites, the series $[Fe_4X_4(YPh)_4]^{2-}$ provides a specific opportunity to explore the potentially general consequences of S/Se substitution on the properties of homologous chalcogen complexes. Discrete transition-metal species suitable for this purpose are not widespread[14] and are primarily confined to mononuclear chelate complexes derived from ligands such as $(CF_3)_2C_2Y_2$[15] and $R_2NCY_2^-$[16] (Y = S, Se). Among tetranuclear clusters other than those reported here, the only established cases of structural homologues are $[(\eta^5\text{-}C_5H_5)_4Fe_4X_4]^{0,1+,2+}$ (X = S,[17,18] Se[19]) and $[Re_4X_4(CN)_{12}]^{4-}$ (X = S, Se).[20]

Experimental Section

All operations and manipulations in the preparation of compounds and their physical measurements were performed under a purified dinitrogen atmosphere.

Preparation of Compounds. $(Et_4N)_2[Fe_4S_4(SPh)_4]$,[10] $(Et_4N)_2[Fe_4S_4(S\text{-}t\text{-}Bu)_4]$,[2] diphenyl diselenide,[21] and ethanolic solutions of sodium hydroselenide[22] were prepared by published procedures.

$(Et_4N)_2[Fe_4S_4(SePh)_4]$. This new salt of the previously reported[3] dianion was synthesized from 0.95 g (0.98 nmol) of $(Et_4N)_2[Fe_4S_4(S\text{-}t\text{-}Bu)_4]$ and 1.87 g (4.9 mmol) of PhSeSePh. The acetonitrile solution was stirred overnight during which time its color changed from greenish brown to dark red-violet. Acetonitrile was then removed under vacuum until crystals began to form. The solution was then warmed to 45 °C, and about 3 volumes of methanol was added. The product was filtered and recrystallized from CH_3CN/MeOH. The crystalline salt was filtered, washed with MeOH, and dried overnight; 0.91 g (76%) of pure product was obtained as red-black crystals. Anal. Calcd for $C_{40}H_{60}Fe_4N_2S_4Se_4$: C, 38.86; H, 4.89; Fe, 18.07; N, 2.27. Found: C, 38.63; H, 4.89; Fe, 17.95; N, 2.21.

$(Me_4N)_2[Fe_4Se_4(SPh)_4]$. The preparation was patterned after the direct synthesis of $[Fe_4S_4(SR)_4]^{2-}$.[2] Addition of 4.87 g (30 mmol) of methanolic $FeCl_3$ to 11.9 g (90 mmol) of NaSPh in the same solvent led to formation of a dark brown solution. A tan precipitate began to form as addition was completed. To this slurry was added a freshly prepared ethanolic solution containing ~30 mmol of NaHSe. The tan solid dissolved, and the solution was stirred ca. 15 h. The solution was then filtered away from a small (<1 g) quantity of off-white

0020-1669/78/1317-1402$01.00/0

powder, and the dianion was crystallized via addition of ~2.5 g (23 mmol) of Me_4NCl in a minimal amount of 70/30 v/v methanol/water. The product was isolated and twice crystallized. Recrystallization entailed dissolving the material in a minimal amount of warm (~45 °C) acetonitrile followed by slow addition of at least 2 volumes of methanol. The black needles thus obtained were washed well with methanol and dried under vacuum for ~12 h, affording 5.4 g (64%) of product. Anal. Calcd for $C_{32}H_{44}Fe_4N_2S_4Se_4$: C, 34.19; H, 3.95; Fe, 19.87; N, 2.49; S, 11.41; Se, 28.09. Found: C, 34.07; H, 4.01; Fe, 20.10; N, 2.52; S, 11.57; Se, 27.70.

$(Et_4N)_2[Fe_4Se_4(S\text{-}t\text{-}Bu)_4]$. This compound was synthesized with sodium *tert*-butylthiolate using the procedure, scale, and stoichiometry of the preceding preparation. The insoluble iron thiolate polymer which formed in the initial step dissolved upon addition of the NaHSe solution. The resulting brown solution was stirred overnight and filtered, and 4.14 g (23.0 mmol) of Et_4NCl was added to the filtrate. The product (4.40 g, 51%) was collected by filtration and purified by recrystallization from 3/1 v/v acetonitrile/methanol, affording fine black crystals which were dried under vacuum. Anal. Calcd for $C_{32}H_{76}Fe_4N_2S_4Se_4$: C, 33.24; H, 6.62; Fe, 19.32; N, 2.42; S, 11.09; Se, 27.31. Found: C, 33.26; H, 6.60; Fe, 19.36; N, 2.35; S, 11.48; Se, 27.36.

$(Et_4N)_2[Fe_4Se_4(SePh)_4]$. $(Et_4N)_2[Fe_4Se_4(S\text{-}t\text{-}Bu)_4]$ (1.23 g, 1.06 mmol) and PhSeSePh (1.65 g, 5.30 mmol) were stirred overnight in acetonitrile solution. Very thin, platelike, black crystals were precipitated by the addition of 2-propanol and were collected by filtration. The filtrate was concentrated under vacuum, and a second crop was collected after addition of 2-propanol. Combination of the two crops gave 0.90 g (60%) of product, which was not recrystallized. Anal. Calcd for $C_{40}H_{60}Fe_4N_2Se_8$: C, 33.74; H, 4.25; Fe, 15.69; N, 1.97; Se, 44.36. Found: C, 33.75; H, 4.16; Fe, 15.44; N, 1.96; Se, 44.12.

All selenium-containing compounds are less stable than their sulfur-containing counterparts and should be handled under strictly anaerobic conditions in solutions maintained at or near room temperature. Observations suggest that $[Fe_4Se_4(SePh)_4]^{2-}$ is the least stable species, and heating or prolonged standing of its solutions have led to separation of intractable black solids.

Physical Measurements. Electronic absorption spectra were measured using a Cary Model 14 or 17 recording spectrophotometer. Polarography was performed on a Princeton Applied Research Model 170 electrochemistry system; cyclic voltammetry and preparative electrochemical reductions utilized equipment described previously.[8] A glassy carbon disk (PAR 9333) served as a working electrode. All quoted potentials were determined vs. the saturated calomel electrode at ~25 °C. Preparative reductions were performed in an H-type cell with two sintered glass disks to separate the working and auxiliary compartments, a platinum gauze working electrode, and a silver wire isolated with an asbestos fiber contact which served as a pseudo reference electrode. Reductions of $[Fe_4X_4(YPh)_4]^{2-}$ species to the corresponding trianions were monitored coulometrically and by cyclic voltammetry at a carbon disk in the working compartment. All electrochemical experiments were performed under an argon atmosphere using solutions containing 0.05 M $(n\text{-}Bu_4N)(BF_4)$ as supporting electrolyte. Electron paramagnetic resonance experiments were carried out with a Varian E-12 spectrometer operating at ca. 9.21 GHz and equipped with an Air Products Model LT-3-110 Helitran refrigerator and a Model APD-B temperature controller. Solutions of the species $[Fe_4X_4(YPh)_4]^{3-}$ were generated electrochemically in DMF or acetonitrile containing supporting electrolyte. Solutions were frozen and EPR spectra recorded at 4.2–20 K within 30 min after preparation. Spectra were run at modulation frequencies between 10^3 and 10^5 Hz as a check for fast passage effects, but line shapes were found to be invariant over this range. Acetonitrile was distilled from $KMnO_4/K_2CO_3$, from P_2O_5, and again from P_2O_5 just prior to use. After removal of water as the benzene azeotrope, DMF was shaken successively with P_2O_5 and KOH and then distilled from BaO at 60 °C (20 mmHg). Magnetic measurements were made with a Superconducting Technology SQUID-type susceptometer calibrated with a constant-current coil.

Crystal Data for $(Me_4N)_2[Fe_4Se_4(SPh)_4]$. X-ray diffraction studies were carried out on a Syntex $P2_1$ four-circle automated diffractometer. Air-sensitive black crystals suitable for X-ray analysis were obtained by vapor diffusion of methanol into an acetonitrile solution of the compound. The crystals were mounted in glass capillaries under an inert atmosphere. Precession photographs confirmed that the crystals had orthorhombic diffraction symmetry and that the space group was $P2_12_12_1$ (No. 19). Unit cell dimensions were accurately determined from 15 machine-centered reflections. The 2θ values for the reflections used in the least-squares refinement of the orientation matrix and lattice parameters were in the range 10.6–14.9°. Crystal data are summarized in Table I; this compound is isomorphous with $(Me_4N)_2[Fe_4S_4(SPh)_4]$.

Table I. Summary of Crystal Data, Intensity Collection, and Structure Refinement of $(Me_4N)_2[Fe_4Se_4(SPh)_4]$

Formula	$C_{32}H_{44}Fe_4N_2S_4Se_4$
a, Å	11.930 (3)
b, Å	24.126 (5)
c, Å	14.782 (4)
Cryst system	Orthorhombic
V, Å^3	4254 (3)
Z	4
d_{calcd}, g/cm^3 [a]	1.759
Space group	$P2_12_12_1$
Cryst dimensions,[b] mm	0.35 × 0.40 × 0.45
Cryst faces	$(1\bar{2}0)$, $(\bar{1}20)$, $(01\bar{1})$, $(\bar{1}\bar{1}2)$, $(0\bar{2}\bar{1})$, (100), $(\bar{1}\bar{1}0)$, $(0\bar{1}2)$
Radiation[c]	Mo ($\lambda(K\bar{\alpha})$ 0.710 69 Å)
Absorption coeff, μ, cm^{-1}	52.6
Transmission factor, %	17.0 min, 41.2 max, 26.9 av
Takeoff angle, deg	3.0
Scan speed	1.5–29.3° min^{-1} ($\theta/2\theta$ scan)
Scan range, deg	0.6 below $K\alpha_1$ to 0.6 above $K\alpha_2$
Background/scan time ratio	0.25
Data collected	2θ of 2–25° $\pm h$, $\pm k$, $\pm l$ 2θ of 25–40° $+h$, $+k$, $+l$
Unique averaged data $(F_o^2 > 3\sigma(F_o)^2)$	1701
No. of variables	295
Error in observn of unit wt (e)	1.82
Highest shift/error, final cycle	0.12
R, %	5.5
R_w, %	6.0

[a] Calculated value; experimental density not determined. [b] Irregularly shaped crystal. [c] Mosaic graphite monochromator.

Data Collection and Reduction. The crystal selected for data collection gave ω scans for several low-angle reflections with full widths at half-height of <0.20°. The data collection parameters are given in Table I. Since the crystal was in an acentric space group, a full sphere of data were collected through 25° in 2θ. Only the positive octant of data were collected above 25° in 2θ. Three standards were collected every 60 reflections and their intensities showed no significant fluctuation or evidence of decomposition.

The processing of the data was carried out as described previously.[9a] An analytical absorption correction was applied to the complete set (see Table I for relevant parameters). The equivalent data which reflected the strict 222 symmetry of the acentric group were averaged, thus resulting in 1701 reflections with $F^2 > 3\sigma(F^2)$ including Friedel pairs. This data set was used in the subsequent refinement of the structure.

Structure Solution and Refinement. The coordinates for the four Fe, four Se, and four S atoms were taken from the $(Me_4N)_2[Fe_4S_4(SPh)_4]$ structure.[3] Isotropic refinement of these 12 atoms led to $R_w = 0.237$. Coordinates of C and N atoms were determined from a subsequent difference Fourier map. Isotropic full-matrix least-squares refinement of these coordinates, using statistical weighting as described previously,[9a,23] gave R_W of 0.088. Inversion of this set of coordinates generated the enantiomorph which refined to R_w of 0.077. Inspection of individual Friedel pairs unambiguously confirmed that the second set of coordinates was correct. Anisotropic refinement of the 12 heavy atoms in the core gave $R = 0.057$ and $R_w = 0.061$. Because of the limited number of observations, the anisotropic refinement was extended to include only the carbon atom attached to the sulfur atom in each ring, one entire cation, and the nitrogen atom of the second cation. The final cycles included fixed contributions for the phenyl ring hydrogen atoms whose positions were calculated assuming trigonal geometry and C–H distances of 1.0 Å. The hydrogen atoms were assigned temperature factors approximately equal to the average of the ring carbon atoms. The final cycle converged to $R = 0.055$ and $R_w = 0.060$. The final error in an observation of unit weight was 1.82 electrons. A final difference Fourier map showed no peaks greater than about 20% of the height of a carbon atom.

Table II. Positional and Thermal Parameters for $(Me_4N)_2[Fe_4Se_4(SPh)_4]$ (Anion Only)

Atom	x	y	z	β_{11}[a]	β_{22}	β_{33}	β_{12}	β_{13}	β_{23}
Fe(1)	0.8178 (3)	0.6807 (2)	0.5969 (3)	0.0071 (4)	0.002 42 (9)	0.0069 (3)	0.0009 (4)	0.0019 (6)	0.0006 (3)
Fe(2)	0.9003 (3)	0.6500 (1)	0.7655 (3)	0.0062 (3)	0.002 06 (9)	0.0065 (3)	0.0007 (3)	−0.0015 (6)	0.0001 (3)
Fe(3)	0.6732 (3)	0.6381 (1)	0.7257 (2)	0.0063 (4)	0.002 21 (9)	0.0055 (2)	−0.0009 (3)	−0.0008 (6)	−0.0006 (3)
Fe(4)	0.7626 (3)	0.7427 (2)	0.7519 (2)	0.0070 (3)	0.002 11 (9)	0.0068 (2)	0.0002 (3)	0.0023 (6)	−0.0007 (3)
Se(1)	0.7488 (2)	0.6704 (1)	0.8649 (2)	0.0091 (3)	0.002 23 (6)	0.0057 (2)	−0.0004 (3)	0.0000 (5)	−0.0003 (2)
Se(2)	0.6369 (2)	0.7169 (1)	0.6298 (2)	0.0071 (3)	0.002 90 (7)	0.0066 (2)	0.0017 (3)	−0.0010 (4)	0.0016 (2)
Se(3)	0.9461 (2)	0.7359 (1)	0.6885 (2)	0.0072 (3)	0.002 32 (7)	0.0083 (2)	−0.0008 (3)	0.0007 (4)	0.0002 (2)
Se(4)	0.8216 (3)	0.5873 (1)	0.6553 (2)	0.0097 (3)	0.002 07 (6)	0.0066 (2)	0.0012 (3)	−0.0007 (5)	−0.0013 (2)
S(1)	0.8859 (6)	0.6913 (3)	0.4560 (4)	0.0080 (8)	0.003 6 (2)	0.0059 (5)	−0.0010 (7)	0.002 (1)	0.0004 (6)
S(2)	1.0607 (6)	0.6235 (3)	0.8387 (6)	0.0074 (8)	0.003 6 (2)	0.0099 (6)	−0.0007 (7)	−0.001 (1)	0.0032 (7)
S(3)	0.5047 (7)	0.5960 (3)	0.7549 (6)	0.0080 (7)	0.003 7 (2)	0.0082 (5)	−0.0048 (7)	0.001 (1)	0.0014 (7)
S(4)	0.7180 (6)	0.8148 (3)	0.8425 (5)	0.0117 (8)	0.001 8 (2)	0.0067 (5)	0.0003 (6)	0.004 (1)	−0.0008 (5)

[a] The form of the anisotropic thermal ellipsoid is $\exp[-(\beta_{11}h^2 + \beta_{22}k^2 + \beta_{33}l^2 + \beta_{12}hk + \beta_{13}hl + \beta_{23}kl)]$. [b] Estimated standard deviations in parentheses in this and succeeding tables.

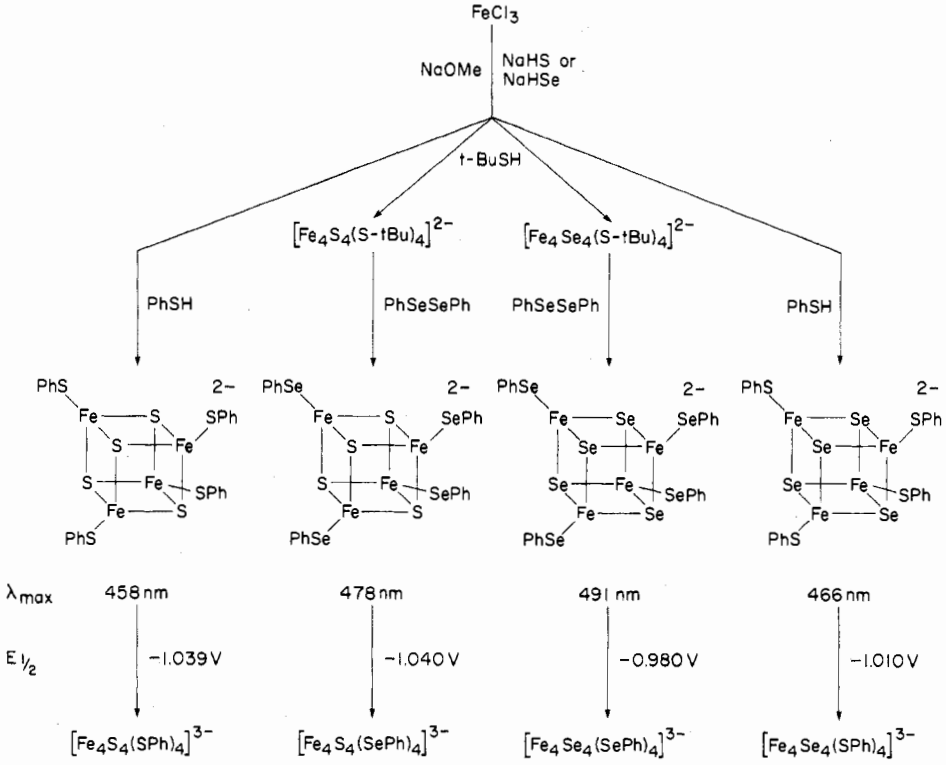

Figure 1. Synthesis and properties of $[Fe_4X_4(YPh)_4]^{2-}$ complexes (X, Y = S, Se); spectra and potentials refer to DMF solutions.

The following results are tabulated: positional and thermal parameters (Table II); bond distances and angles (Table III); best weighted least-squares planes (Table IV); root-mean-square amplitudes of thermal vibration (Table V). Because the phenyl rings of the anion and the Me_4N^+ cations are structurally unexceptional and do not bear directly on the most important structural feature, the $Fe_4Se_4S_4$ cluster of the anion, data for only this cluster are included in Tables II–V. Deposited elsewhere[24] are positional and thermal parameters of the cations and phenyl rings (Table VI), a listing of values of $10|F_o|$ and $10|F_c|$ (Table VII), and calculated H atom positions (Table VIII). Selected structural features of $[Fe_4Se_4(SPh)_4]^{2-}$ and $[Fe_4S_4(SPh)_4]^{2-}$[3] are compared in Table IX.

Results and Discussion

Synthesis of the Series $[Fe_4X_4(YPh)_4]^{2-}$. The synthetic scheme leading to the four members of this series, in which chalcogenide atoms in sets of four occupy bridging and terminal ligand positions, is depicted in Figure 1. Direct synthesis of $[Fe_4S_4(SPh)_4]^{2-}$ by the means indicated has already been demonstrated;[2] it and the other tetranuclear dianions are readily isolated as quaternary ammonium salts soluble in polar organic solvents. Employment of NaHSe[22] in the reaction mixture afforded straightforward synthesis of the Fe_4Se_4 core in the form of $[Fe_4Se_4(SPh)_4]^{2-}$, whose Me_4N^+ salt was obtained in 64% yield after purification. Analogous reactions but with *tert*-butylthiol afforded salts of $[Fe_4S_4(S\text{-}t\text{-}Bu)_4]^{2-}$[2] and $[Fe_4Se_4(S\text{-}t\text{-}Bu)_4]^{2-}$ (51%). Terminal selenium ligation was readily introduced by smooth reaction of these dianions with diphenyl diselenide in acetonitrile solution, giving $[Fe_4S_4(SePh)_4]^{2-}$ (76%) and the fully selenium-substituted species $[Fe_4Se_4(SePh)_4]^{2-}$ (60%). This procedure avoids the use of malodorous benzeneselenol, which in direct synthesis[2] or ligand exchange[3] with $[Fe_4X_4(S\text{-}t\text{-}Bu)_4]^{2-}$ is expected to afford the same products. All four dianions can be readily reduced electrochemically to $[Fe_4X_4(YPh)_4]^{3-}$ (vide infra). Chemical reduction and isolation of selenium-containing trianions, similar to the procedure affording salts of $[Fe_4S_4(SPh)_4]^{3-}$,[8] were not pursued.

Description of the Structure of $(Me_4N)_2[Fe_4Se_4(SPh)_4]$. With a precise structure of $[Fe_4S_4(SPh)_4]^{2-}$ already determined,[3] the most significant structural objective remaining in the $[Fe_4X_4(YPh)_4]^{2-}$ series is stereochemical definition of the Fe_4Se_4 core. The title compound was selected for this purpose and was found to crystallize in an orthorhombic space group (Table I) isomorphous with that of $(Me_4N)_2[Fe_4S_4(SPh)_4]$.[3] Structural and thermal parameter data for the $Fe_4Se_4S_4$ cluster of the dianion are given in Tables II, III, and V; least-squares

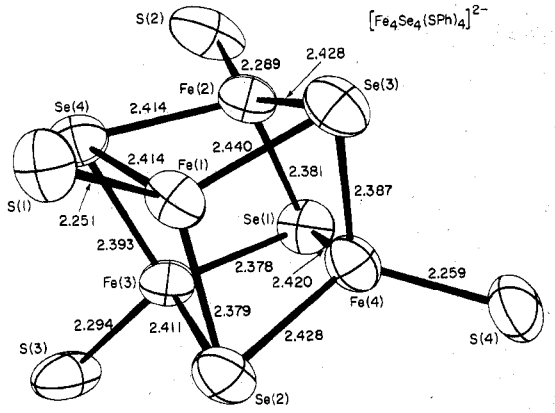

Figure 2. Structure of $[Fe_4Se_4(SPh)_4]^{2-}$, including the atom-labeling scheme, selected bond distances, and 50% probability ellipsoids of thermal vibration; phenyl rings omitted.

planes of the Fe_4Se_4 core and positional deviations therefrom are listed in Table IV.[24] The dianion cluster structure is depicted in Figure 2, from which the essential cubane-type geometry of I is immediately evident. $[Fe_4Se_4(SPh)_4]^{2-}$ joins $[Fe_4S_4(SCH_2Ph)_4]^{2-}$,[2] $[Fe_4S_4(SPh)_4]^{2-}$,[3] $[Fe_4S_4Cl_4]^{2-}$,[9a] and $[Fe_4S_4(SCH_2CH_2CO_2)_4]^{6-}$[4] in a structurally related series whose members possess isoelectronic $[Fe_4X_4]^{2+}$ cores. While a cubane-type core is now an unexceptional inorganic stereochemical unit,[25] only $[(\eta^5\text{-}C_5H_5)_4Fe_4Se_4]^{0,2+}$[19] and $[Re_4Se_4(CN)^{12}]^{4-}$[20] have been shown previously by X-ray diffraction to contain M_4Se_4 cores.[26]

It is evident from Figure 2 and the metrical data of Table III that the core of $[Fe_4Se_4(SPh)_4]^{2-}$ departs from idealized cubic (T_d-$\bar{4}3m$) symmetry toward the tetragonal point group D_{2d}-$\bar{4}2m$ where the (noncrystallographically imposed) $\bar{4}$ axis passes through the upper and lower faces of the polyhedron. The same distortion is found in $[Fe_4S_4(SCH_2Ph)_4]^{2-}$,[2,29] $[Fe_4S_4(SPh)_4]^{2-}$,[3] $[Fe_4S_4(SCH_2CH_2CO_2)_4]^{6-}$,[4] and $[Fe_4S_4Cl_4]^{2-}$[9a] and is of a form such that the core is compressed along this axis. Because of previous, more detailed considerations of these structures,[2,6,29] this discussion is limited to descriptions of the more important structural features. (i) Each face of the Fe_4Se_4 core is a rhomb (mean Se–Fe–Se and Fe–Se–Fe angles of 106.4 and 70.6°, respectively) which is puckered (Table IV, planes 1–6). (ii) None of the planes 7–12 passing through the core is perfect within experimental error. (iii) Core distances and angles under D_{2d} symmetry divide into the sets Fe–Fe, Se···Se (2 + 4), Fe–Se (4 + 8), and Fe–Fe–Fe, Se–Se–Se, Se–Fe–Se, Fe–Se–Fe (4 + 8). Of these parameters Se···Se and Fe–Se distances[30] and Se–Se–Se angles more clearly resolve into the expected subsets. (iv) The Fe–Se distances divide into four short (mean 2.385 (2) Å) and eight long (mean 2.417 (5) Å) which are approximately parallel and perpendicular, respectively, to the $\bar{4}$ axis. (v) The Se_4 portion of the core strongly deviates from tetrahedral symmetry and together with the Fe–Se distances most clearly reflects the close approach of the core to overall D_{2d} symmetry. The nonbonding Se···Se distances occur as two long (mean 3.901 Å) and four short (mean 3.827 (9) Å) which are approximately perpendicular and parallel, respectively, to the $\bar{4}$ axis. (vi) The $Fe_4Se_4S_4$ cluster is devoid of symmetry, as may be seen from (ii) and the large variation in S–Fe–Se angles (97.4–120.2°).

Structural features (i)–(vi) are common to all cluster dianions I,[2-4,9a] but with some differences observed in the symmetry-required divisions of angles into experimentally resolvable subsets, in the degree of distortion of the Fe_4 unit from tetrahedral to tetragonal, and in the spread of S–Fe–X angles. The comparison of selected structural parameters of $[Fe_4S_4(SPh)_4]^{2-}$ and $[Fe_4Se_4(SPh)_4]^{2-}$ in Table IX serves to illustrate the close structural relationship between isoelectronic

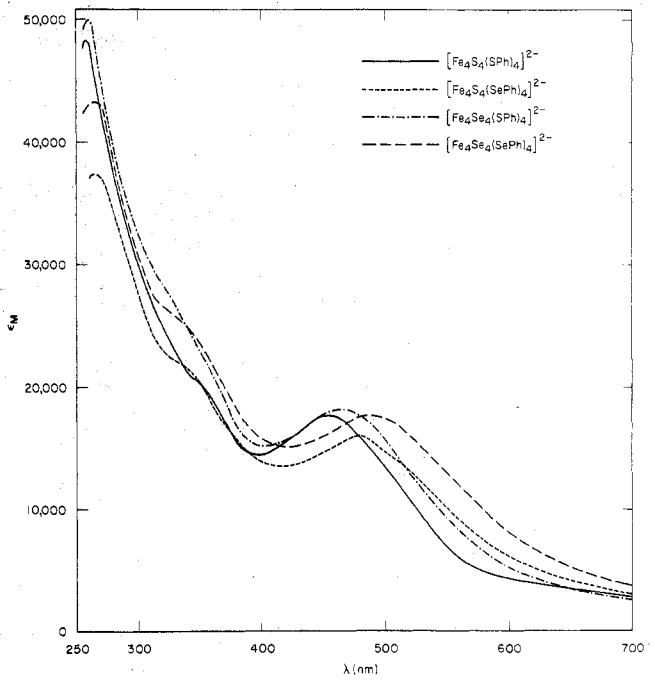

Figure 3. Visible–ultraviolet electronic absorption spectra of the series $[Fe_4X_4(YPh)_4]^{2-}$ in DMF solution at ~25 °C.

complexes which differ only in bridging chalcogenide. The Fe–X bond distance difference of 0.11 Å compares favorably with M–Y(X) distances (Y(X) = S, Se) in the following sets of compounds: $M(Y_2CNEt_2)_2$ (M = Ni, Cu, Zn), 0.11 Å (mean value);[31] $[Ni(Y_2CN\text{-}n\text{-}Bu_2)_3]^+$, 0.13 Å;[32] $Mo(Y_2C_2R_2)_3$, 0.16 Å;[33] As_4X_4 (D_{2d}), 0.14 Å;[34] $Fe_3X_2(CO)_9$, 0.12 Å;[35] $[(\eta^5\text{-}C_5H_5)_4Fe_4X_4]^{0,2+}$, 0.10–0.15 Å.[17-19] These values in turn are compatible with the 0.13-Å difference in selenium and sulfur covalent radii.[36] The difference in Fe–X–Fe angles reflects the usual trend toward smaller angles when selenium rather than sulfur is the central atom. Examples are found with As_4X_4 (3.7°),[34] $Fe_3X_2(CO)_9$ (2–3°),[35] and $[(\eta^5\text{-}C_5H_5)_4Fe_4X_4]^{0,2+}$ (2–4°).[17-19] Hence the dimensional variations between $[Fe_4S_4(SPh)_4]^{2-}$ and $[Fe_4Se_4(SPh)_4]^{2-}$ are fully accountable in terms of established relative structural effects of the two chalcogenides.

Electronic Absorption Spectra. The spectra of $[Fe_4S_4(SR)_4]^{2-}$ complexes are dominated by two bands in the 300–500-nm region[5,10] which, based on intensities and the results of a SCF–Xα–SW electronic structural model for $[Fe_4S^*_4(SMe)_4]^{2-}$,[37] have been assigned as charge-transfer transitions from orbitals with Fe–S*–S character to an antibonding, partially occupied Fe_4 core orbital 3d-like in character. Solution spectra of the $[Fe_4X_4(YPh)_4]^{2-}$ series are shown in Figure 3 and data are collected in Table X. A well-resolved visible feature (the lowest energy intense band in each spectrum) and a shoulder in the vicinity of 330 nm are common to all species and are assigned as charge-transfer bands. The intense ultraviolet bands arise from intraligand transitions. Selenium substitution produces red spectral shifts of the visible bands which are larger for PhSe/PhS terminal ligand change (800, 1100 cm^{-1}) than for Fe_4Se_4/Fe_4S_4 core alteration (300, 600 cm^{-1}). The features appearing as shoulders are not sufficiently resolved to follow their energy changes with certainty. The largest energy difference (1400 cm^{-1}) is found between $[Fe_4S_4(SPh)_4]^{2-}$ and the fully substituted complex $[Fe_4Se_4(SePh)_4]^{2-}$. These results are qualitatively consistent with prior observations that replacement of ligated sulfur with selenium in otherwise identical complexes appears to have the general effect of decreasing ligand → metal charge-transfer energies.[16,38-41] In such cases

Table III. Bond Distances (Å) and Angles (deg) for $[Fe_4Se_4(SPh)_4]^{2-}$ ($[Fe_4Se_4S_4]$ Cluster Only)

Distances			
Fe–S			
Fe(1)–S(1)	2.251 (7)	Fe(4)–S(4)	2.259 (7)
Fe(2)–S(2)	2.289 (8)	Mean	2.273 (7)[a]
Fe(3)–S(3)	2.294 (8)		
Fe–Se			
Fe(1)–Se(2)	2.379 (4)	Fe(4)–Se(3)	2.387 (4)
Fe(2)–Se(1)	2.381 (4)	Mean	2.385 (2)
Fe(3)–Se(4)	2.393 (4)		
Fe(1)–Se(3)	2.440 (4)	Fe(3)–Se(2)	2.411 (4)
Fe(1)–Se(4)	2.414 (4)	Fe(4)–Se(1)	2.420 (4)
Fe(2)–Se(3)	2.428 (4)	Fe(4)–Se(2)	2.428 (4)
Fe(2)–Se(4)	2.414 (4)	Mean	2.417 (5)
Fe(3)–Se(1)	2.378 (4)	Mean (of 12)	2.406
Fe···Se			
Fe(1)–Se(1)	4.054 (4)	Fe(4)–Se(4)	4.075 (4)
Fe(2)–Se(2)	4.063 (4)	Mean	4.063 (3)
Fe(3)–Se(3)	4.058 (4)		
Fe···Fe			
Fe(1)–Fe(2)	2.780 (5)	Mean	2.773
Fe(3)–Fe(4)	2.766 (5)		
Fe(1)–Fe(3)	2.767 (5)	Fe(2)–Fe(4)	2.783 (4)
Fe(1)–Fe(4)	2.815 (5)	Mean	2.788 (7)
Fe(2)–Fe(3)	2.787 (4)	Mean (of 6)	2.783
Se···Se			
Se(1)–Se(2)	3.889 (4)	Mean	3.901
Se(3)–Se(4)	3.913 (3)		
Se(1)–Se(3)	3.852 (4)	Se(2)–Se(4)	3.845 (3)
Se(1)–Se(4)	3.793 (4)	Mean	3.827 (9)
Se(2)–Se(3)	3.817 (4)	Mean (of 6)	3.852
Angles			
Fe–Se–Fe			
Fe(2)–Se(1)–Fe(4)	70.84 (12)	Fe(4)–Se(3)–Fe(1)	71.33 (13)
Fe(2)–Se(1)–Fe(3)	71.68 (13)	Fe(2)–Se(3)–Fe(1)	69.65 (13)
Fe(4)–Se(1)–Fe(3)	70.40 (13)	Fe(3)–Se(4)–Fe(1)	70.29 (13)
Fe(1)–Se(2)–Fe(3)	70.56 (13)	Fe(3)–Se(4)–Fe(2)	70.87 (12)
Fe(1)–Se(2)–Fe(4)	71.70 (14)	Fe(1)–Se(4)–Fe(2)	70.32 (13)
Fe(3)–Se(2)–Fe(4)	69.73 (12)	Mean	70.55
Fe(4)–Se(3)–Fe(2)	70.60 (13)		
S–Fe–Se			
S(1)–Fe(1)–Se(2)	118.3 (2)	S(3)–Fe(3)–Se(2)	107.6 (2)
S(1)–Fe(1)–Se(3)	103.0 (2)	S(3)–Fe(3)–Se(4)	120.2 (2)
S(1)–Fe(1)–Se(4)	115.5 (2)	S(4)–Fe(4)–Se(1)	97.4 (2)
S(2)–Fe(2)–Se(1)	113.6 (2)	S(4)–Fe(4)–Se(2)	119.5 (2)
S(2)–Fe(2)–Se(3)	105.8 (2)	S(4)–Fe(4)–Se(3)	120.0 (2)
S(2)–Fe(2)–Se(4)	118.0 (2)	Mean	112.3
S(3)–Fe(3)–Se(1)	108.3 (2)		
Se–Fe–Se			
Se(2)–Fe(1)–Se(3)	104.8 (2)	Se(1)–Fe(3)–Se(4)	105.3 (1)
Se(2)–Fe(1)–Se(4)	106.7 (2)	Se(2)–Fe(3)–Se(4)	106.3 (1)
Se(3)–Fe(1)–Se(4)	107.5 (2)	Se(1)–Fe(4)–Se(2)	106.7 (2)
Se(1)–Fe(2)–Se(3)	106.4 (2)	Se(1)–Fe(4)–Se(3)	106.5 (2)
Se(1)–Fe(2)–Se(4)	104.6 (2)	Se(2)–Fe(4)–Se(3)	104.9 (2)
Se(3)–Fe(2)–Se(4)	107.9 (2)	Mean	106.4
Se(1)–Fe(3)–Se(2)	108.6 (2)		
Fe–Fe–Fe			
Fe(4)–Fe(1)–Fe(3)	59.41 (12)	Fe(1)–Fe(4)–Fe(2)	59.55 (12)
Fe(4)–Fe(2)–Fe(3)	59.56 (12)	Mean	59.65
Fe(1)–Fe(3)–Fe(2)	60.08 (12)		
Fe(4)–Fe(1)–Fe(2)	59.65 (12)	Fe(1)–Fe(3)–Fe(4)	61.16 (12)
Fe(3)–Fe(1)–Fe(2)	60.32 (11)	Fe(2)–Fe(4)–Fe(3)	60.29 (12)
Fe(4)–Fe(2)–Fe(1)	60.80 (11)	Fe(1)–Fe(4)–Fe(3)	59.43 (12)
Fe(3)–Fe(2)–Fe(1)	59.61 (12)	Mean	60.18
Fe(2)–Fe(3)–Fe(4)	60.15 (11)	Mean (of 12)	60.00
Se–Se–Se			
Se(3)–Se(1)–Se(4)	61.57 (7)	Se(1)–Se(4)–Se(2)	61.20 (7)
Se(3)–Se(2)–Se(4)	61.43 (7)	Mean	61.28
Se(1)–Se(3)–Se(2)	60.93 (7)		
Se(2)–Se(1)–Se(3)	59.09 (7)	Se(2)–Se(3)–Se(4)	59.64 (7)

Table III (*Continued*)

	Angles (*Continued*)		
Se(2)-Se(1)-Se(4)	60.05 (6)	Se(1)-Se(4)-Se(3)	59.95 (7)
Se(1)-Se(2)-Se(3)	59.98 (7)	Se(2)-Se(4)-Se(3)	58.93 (6)
Se(1)-Se(2)-Se(4)	58.74 (6)	Mean	59.36
Se(1)-Se(3)-Se(4)	58.48 (6)	Mean (of 12)	60.00
	S-C (Ring)[b]		
S(1)-C(1)R(1)	1.76 (2)	S(4)-C(1)R(4)	1.75 (2)
S(2)-C(1)R(2)	1.74 (2)	Mean	1.74
S(3)-C(1)R(3)	1.69 (3)		
	Fe-S-C (Ring)[b]		
Fe(1)-S(1)-C(1)R(1)	105.9 (7)	Fe(4)-S(4)-C(1)R(4)	104.4 (6)
Fe(2)-S(2)-C(1)R(2)	101.5 (8)	Mean	105.7
Fe(3)-S(3)-C(1)R(3)	110.9 (9)		

[a] If given, the value in parentheses is the standard deviation as estimated from the variances among the averaged values. The estimated standard deviation of the mean is not given for any angular quantity, as the variations exceed those expected from a sample taken from the same population. [b] Rings numbered according to S atoms to which they are attached.

Table IV. Best Weighted Least-Squares Planes for $[Fe_4Se_4(SPh)_4]^{2-}$

$Ax + By + Cz - D = 0$ (Orthogonalized Coordinates, Å)

Plane no.	*A*	*B*	*C*	*D*	Plane no.	*A*	*B*	*C*	*D*
1	−0.5316	−0.4597	−0.7114	−18.7544	7	0.6316	0.3728	−0.6798	4.9026
2	−0.5167	−0.4446	−0.7317	−21.0276	8	−0.5973	0.7991	−0.0677	6.7404
3	0.8586	−0.2975	−0.4175	0.0314	9	−0.3835	−0.9127	−0.1410	−20.0026
4	0.8554	−0.2984	−0.4234	−2.4749	10	−0.3518	0.2726	−0.8955	−8.2529
5	0.0267	0.8433	−0.5368	7.1742	11	−0.9728	−0.1029	−0.2076	−13.0059
6	0.0210	0.8461	−0.5326	9.6811	12	0.2504	−0.5287	−0.8110	−14.8043

Distances (Å) from Planes

	Plane											
Atom	1	2	3	4	5	6	7	8	9	10	11	12
Fe(1)	−0.258[a]		−0.225			−0.281		−0.042	0.028		−0.006	
Fe(2)		0.227	−0.200		0.263		0.034		−0.025			0.025
Fe(3)	−0.224			0.210	0.265			0.038		0.017		−0.025
Fe(4)		0.228		0.204		0.249	−0.034			−0.017	0.005	
Se(1)		−0.134		−0.123	−0.158			−0.016	0.010		−0.002	
Se(2)	0.141			−0.128		0.155	0.015		−0.011			0.011
Se(3)		−0.145	0.127			0.158		0.017		0.008		−0.012
Se(4)	0.140		0.125		0.163		−0.015			−0.007	0.002	

[a] The estimated deviations in distances from the planes are ±0.003 Å or ±0.004 Å for all distances.

Table V. Root-Mean-Square Amplitudes of Thermal Vibration (Å)[a]

Atom	Min	Intermed	Max
Fe(1)	0.218	0.261	0.288
Fe(2)	0.204	0.250	0.271
Fe(3)	0.206	0.244	0.263
Fe(4)	0.215	0.248	0.284
Se(1)	0.246	0.254	0.263
Se(2)	0.211	0.263	0.310
Se(3)	0.223	0.265	0.305
Se(4)	0.228	0.262	0.290
S(1)	0.226	0.267	0.327
S(2)	0.229	0.281	0.371
S(3)	0.197	0.300	0.361
S(4)	0.219	0.256	0.313

[a] Data for $Fe_4Se_4S_4$ cluster only.

Jørgensen's theory of charge-transfer spectra,[42] utilizing optical electronegativities χ_{opt}, predicts that energy differences of the first allowed band for complexes of the same metal should be given by ΔE_{CT} (cm^{-1}) = 30000[χ_{opt}(S) − χ_{opt}(Se)]. Various estimates of the difference term using data for complexes terminally ligated by selenium lead to values of $\lesssim$0.1.[16a,c,38-41] Results for $[Fe_4S_4(YPh)_4]^{2-}$ (Y = S, Se) indicate that the optical electronegativity difference between sulfur and selenium in YPh is even smaller, viz., 0.03–0.04.

Electrochemical Results. The cyclic voltammograms in Figure 4 serve to define the essential features of the cathodic electrochemistry of the $[Fe_4X_4(YPh)_4]^{2-}$ series. All species exhibit a well-defined 2−/3− step whose ΔE_p and i_p^c/i_p^a values (from −0.5 to −1.3 V scans) indicate close approach to electrochemical reversibility and a 3−/4− step which appears chemically irreversible owing to the instability of the tetraanions. These results accord with the usual behavior of $[Fe_4S_4(SR)_4]^{2-}$ complexes.[5,10] Preparative reduction experiments reveal that reduced selenium-containing tetramers are not as stable as $[Fe_4S_4(SPh)_4]^{3-}$. Whereas in DMF solution $[Fe_4S_4(SPh)_4]^{2-}$ is 90% reduced with 1.0 equiv of electrons in 45 min, $[Fe_4Se_4(SPh)_4]^{2-}$ and $[Fe_4S_4(SePh)_4]^{2-}$ under similar conditions were 80% reduced with 1.1 equiv and $[Fe_4Se_4$-

Table IX. Comparison of Selected Structural Parameters of $[Fe_4S^*_4(SPh)_4]^{2-}$ and $[Fe_4Se_4(SPh)_4]^{2-}$

	$[Fe_4X_4(SPh)_4]^{2-}$	
Parameter	X = S* [a,b]	X = Se[b,c]
Fe-S[j]	2.263	2.273
Fe-X	2.267 (4), 2.296 (8)[d]	2.385 (4), 2.417 (8)[e]
Fe···Fe	2.730 (2), 2.739 (4)[f]	2.773 (2), 2.788 (4)[g]
S-Fe-X[k]	115.1	112.3
Fe-X-Fe	73.50	70.55
X-Fe-X	104.3	106.4
Fe-Fe-Fe	59.79 (4), 60.11 (8)[h]	59.65 (4), 60.18 (8)[i]

[a] Me_4N^+ salt; data from ref 3. [b] Number of values averaged indicated when two distances or angles are given. [c] This work. [d–i] Mean of all values: *d*, 2.286; *e*, 2.406; *f*, 2.736; *g*, 2.783; *h*, 59.99; *i*, 60.00. [j] Distances in angstroms. [k] Angles in degrees.

Table X. Electronic Spectral and Redox Potential Data for the Series $[Fe_4X_4(YPh)_4]^{2-}$ in DMF Solution

Species[a]	λ_{max}, nm (ϵ_M, M^{-1} cm^{-1})			E_1[b]	E_2[b]
$[Fe_4S_4(SPh)_4]^{2-}$	260 (48 200[c])	345 (sh, 20 700)	458 (17 600)	−1.039	−1.748
$[Fe_4S_4(SePh)_4]^{2-}$	267 (37 100)	330 (sh, 22 300)	476 (15 800)	−1.040	−1.720
$[Fe_4Se_4(SPh)_4]^{2-}$	260 (50 100)	320 (sh, 28 300)	466 (18 100)	−1.010	−1.615
$[Fe_4Se_4(SePh)_4]^{2-}$	263 (43 300)	330 (sh, 25 800)	490 (17 700)	−0.980	−1.540

[a] $[Fe_4Se_4(S\text{-}t\text{-}Bu)_4]^{2-}$: 260 (19 500); 315 (18 600); 418 (16 300). [b] Potentials (V) from differential-pulse polarography vs. SCE; $E_1 = E(2-/3-)$, $E_2 = E(3-/4-)$. [c] Previous values in DMF, Me_2SO, and acetonitrile solutions fall in the range 41 400–45 000.[5,8,10]

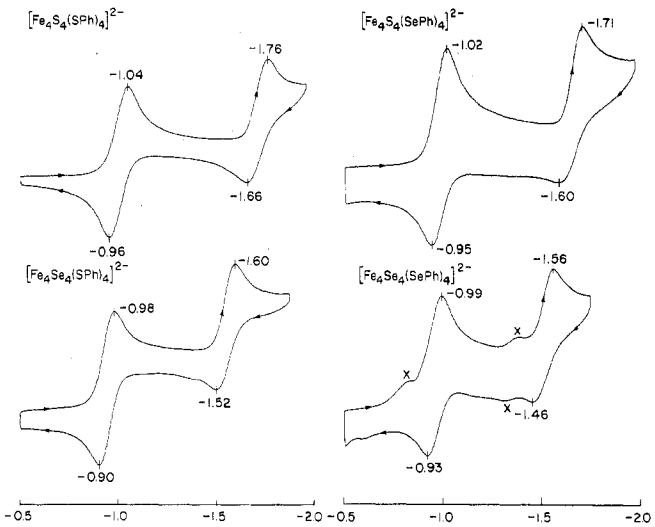

Figure 4. Cyclic voltammograms of the series $[Fe_4X_4(YPh)_4]^{2-}$ at a carbon disk electrode and 50-mV/s scan rate in acetonitrile solution at ~25 °C; × = unidentified impurity.

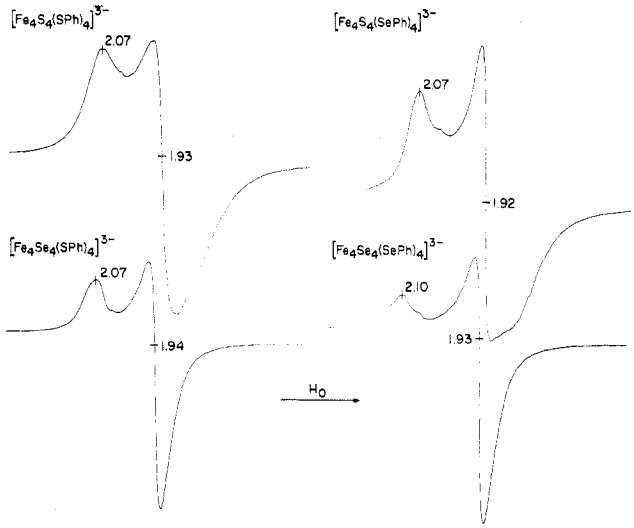

Figure 5. EPR spectra of the series $[Fe_4X_4(YPh)_4]^{3-}$ in DMF. All samples were electrochemically generated except for $[Fe_4S_4(SPh)_4]^{3-}$, which was used as its isolated Et_4N^+ salt.[8] Spectra were recorded at X-band frequencies, 3-mW microwave power, and 4.2 K except for $[Fe_4Se_4(SPh)_4]^{3-}$, whose spectrum was obtained at 20 K.

$(SePh)_4]^{2-}$ was only 60% reduced to the trianion stage with 1.2 equiv. Extents of reduction were determined from cyclic voltammetric peak heights; $[Fe_4Se_4(SePh)_4]^{2-}$ was reduced at 0 °C owing to its lesser stability. In contrast to the other two selenium-containing tetramers the latter complex decomposed when preparative reductions were attempted in acetonitrile solution.

Potentials for the 2−/3− and 3−/4− reduction steps in DMF solution were accurately determined by differential-pulse polarography and are listed in Table X. Except for the $[Fe_4S_4(SPh)_4]^{2-/3-}/[Fe_4S_4(SePh)_4]^{2-/3-}$ comparison selenium substitution produces positive potential shifts in both reduction steps, with larger shifts observed upon selenium introduction into the Fe_4X_4 core. For the physiologically relevant 2−/3− process[6] potential changes are very small and amount to +29, +60 mV and −1, +30 mV at parity of terminal ligand and core, respectively. Prior redox potential data reflecting the effects of S/Se substitution in homologous complexes are sparse but consistent with the present results. Thus for the one-electron couples in the dithiolene/diselolene series $[M(Y_2S_2(CF_3)_2)_{2,3}]^{z}$[15] and $[(\eta^5\text{-}C_5H_5)_4Fe_4X_4]^{z}$[18b,19,43] potentials are usually 30–250 mV more positive for the selenium species, with the large majority of values near the lower end of this range.

Magnetism and EPR Results. The magnetic susceptibility of $(Me_4N)_2[Fe_4Se_4(SPh)_4]$ was determined over the range 4.2–338 K. After impurity[44] and diamagnetic corrections the susceptibility per tetramer increased at all temperatures above 65 K, yielding a $\chi_t(T)$ behavior which is uniformly displaced from that of $[Fe_4S_4(SPh)_4]^{2-}$ by an amount equal to the difference in the apparent temperature-independent paramagnetism calculated from the impurity correction.[44] The following results for $[Fe_4S_4(SPh)_4]^{2-}$ and $[Fe_4Se_4(SPh)_4]^{2-}$ [μ_t, μ_B (T, K)] are drawn from a larger body of data: 0.71, 0.97 (100); 1.56, 1.86 (200); 2.17, 2.47 (299); 2.38, 2.67 (338). As in all $[Fe_4S_4L_4]^{2-}$ complexes investigated (L = RS,[45] Cl[9b]) the behavior of $[Fe_4Se_4(SPh)_4]^{2-}$ is indicative of antiferromagnetic interactions which lead to a singlet ground state and low-lying paramagnetic states. Because the shapes of susceptibility vs. temperature curves have only a slight dependence on L,[9b,44] they are determined by core structure. Provided impurity corrections are accurate, the 0.04–0.05-Å increase in Fe···Fe distances and changes in Fe–X–Fe angles in $[Fe_4Se_4(SPh)_4]^{2-}$ (Table VIII) are at least compensated by X = Se vs. S as a mediator for superexchange interactions within (or, equivalently, a determinant of spin-state separations of) the core unit.

EPR spectra of the series $[Fe_4X_4(YPh)_4]^{3-}$ in frozen solutions are depicted in Figure 5. Trianions were electrochemically generated except for $[Fe_4S_4(SPh)_4]^{3-}$, which was used as the Et_4N^+ salt obtained from synthesis.[8] Line shapes are dominantly axial, with an unresolved rhombic component apparent in the spectrum of $[Fe_4S_4(SePh)_4]^{3-}$, and resemble those of reduced 4-Fe sites in ferredoxins whose tertiary structure has been unfolded in aprotic aqueous solvents.[46] The similarities in line shapes and apparent g values are a clear indication of equivalent ground electronic states of all members of the series. The structural and electronic properties of $[Fe_4S_4(SR)_4]^{3-}$ complexes will be fully reported elsewhere.[45]

Selenium in Proteins. Recent summaries[47] of selenium biochemistry have served to focus interest in this element as an essential component of proteins. Of the three currently best defined selenoproteins, glutathione peroxidase,[48] formate dehydrogenase,[47a,49] and glycine reductase,[50] only the second is a metalloprotein (Fe, Mo) and only in the last has the chemical form of selenium (selenocysteine) been definitely identified. In other cases there is a possibility that selenium may occur in another form. Acid-labile selenium (selenide) has been reported in formate dehydrogenase.[49] It has been hypothesized that the selenium content of the laboratory diet of rats may be partially incorporated as selenide at the redox centers of nonheme iron proteins present in liver microsomal fractions and that such proteins are protected against oxidative destruction in vivo by vitamin E.[51] If correct, such proteins

may act as redox couplers to an oxidizing enzyme similar to, e.g., the coupling of putidaredoxin (a 2-Fe protein with site II) to the cytochrome P-450 monooxygenase system.[52]

The results from this and preceding investigations demonstrate the feasibility of selenium-containing 2-Fe and 4-Fe sites in proteins. Reconstitution of apoadrenodoxin,[11] apoputidaredoxin,[12] and apoferredoxin from parsley[13] yields proteins with Fe_2Se_2 cores which, although less stable, are substantially active in standard biological assays. Compared to the native proteins these species exhibit red-shifted absorption spectra and small changes of variable sign in redox potentials (parsley ferredoxin, +38 mV;[53] adrenodoxin, −14 mV;[11] putidaredoxin, −10 mV[54]). Chromophores with similar spectra have been generated in solution from $FeCl_3$, selenous acid, and excess 1,4-butanedithiol.[55] Successful synthesis of $[Fe_4Se_4(SR)_4]^{2-}$ (R = Ph, *t*-Bu), $[Fe_4S_4(SePh)_4]^{2-}$, and $[Fe_4Se_4(SePh)_4]^{2-}$ suggests that bridging by selenide and terminal ligation by selenocysteinate in protein site I are possible. The stability of species with mixed S/Se core and terminal ligands was not investigated. The essentially reversible redox reaction $[Fe_4X_4(YPh)_4]^{2-/3-}$ involves clusters with the same total oxidation levels as in the oxidized/reduced ferredoxin couple.[6] The comparative properties of members of the $[Fe_4X_4(YPh)_4]^{2-/3-}$ series confirm selenium as a fully functional substitute for sulfur. Inasmuch as the only known biological function of protein sites I and II is electron transfer, any natural selection of selenium over sulfur such as might ultimately be demonstrated by protein isolation would presumably be made to alter redox potentials. Taking the data of Table X as a guide, it would appear that selenium incorporation in the core unit of site I would be more suited to this purpose than terminal selenocysteinate binding.

Acknowledgment. This research was supported by National Institutes of Health Grant GM-22352. We thank Professor L. F. Dahl for providing a copy of the thesis cited in ref 19.

Registry No. $(Et_4N)_2[Fe_4S_4(SePh)_4]$, 66303-56-8; $(Me_4N)_2[Fe_4Se_4(SPh)_4]$, 66416-78-2; $(Et_4N)_2[Fe_4Se_4(S\text{-}t\text{-}Bu)_4]$, 66416-77-1; $(Et_4N)_2[Fe_4Se_4(SePh)_4]$, 66416-79-3; $[Fe_4S_4(SPh)_4]^{2-}$, 52325-39-0; $[Fe_4S_4(SePh)_4]^{2-}$, 52885-90-2; $[Fe_4Se_4(SPh)_4]^{2-}$, 66303-43-3; $[Fe_4Se_4(SePh)_4]^{2-}$, 66303-42-2; $[Fe_4S_4(SPh)_4]^{3-}$, 52627-89-1; $[Fe_4S_4(SePh)_4]^{3-}$, 66303-41-1; $[Fe_4Se_4(SPh)_4]^{3-}$, 66303-40-0; $[Fe_4Se_4(SePh)_4]^{3-}$, 66303-39-7; $[Fe_4S_4(SPh)_4]^{4-}$, 66213-39-6; $[Fe_4S_4(SePh)_4]^{4-}$, 66213-38-5; $[Fe_4Se_4(SPh)_4]^{4-}$, 66213-37-4; $[Fe_4Se_4(Se_4Ph)_4]^{4-}$, 66255-43-4; $(Et_4N)_2[Fe_4S_4(S\text{-}t\text{-}Bu)_4]$, 62873-87-4; $[Fe_4Se_4(S\text{-}t\text{-}Bu)_4]^{2-}$, 66303-38-6; PhSeSePh, 1666-13-3.

Supplementary Material Available: Table VI (positional and thermal parameters of the Me_4N^+ cations and phenyl rings of $(Me_4N)_2[Fe_4Se_4(SPh)_4]$), Table VII (listing of values of $10|F_o|$ and $10|F_c|$ for $(Me_4N)_2[Fe_4Se_4(SPh)_4]$), and Table VIII (calculated coordinates of phenyl hydrogen atoms) (12 pages). Ordering information is given on any current masthead page.

References and Notes

(1) (a) National Science Foundation Postdoctoral Fellow, 1976–1977. (b) Alfred P. Sloan Foundation Fellow, 1976–1978.
(2) B. A. Averill, T. Herskovitz, R. H. Holm, and J. A. Ibers, *J. Am. Chem. Soc.*, **95**, 3523 (1973).
(3) L. Que, Jr., M. A. Bobrik, J. A. Ibers, and R. H. Holm, *J. Am. Chem. Soc.*, **96**, 4168 (1974).
(4) $[Fe_4S_4(SCH_2CH_2CO_2)_4]^{6-}$ has the same cluster as the dianions I: H. L. Carrell, J. P. Glusker, R. Job, and T. C. Bruice, *J. Am. Chem. Soc.*, **99**, 3683 (1977).
(5) J. J. Mayerle, S. E. Denmark, B. V. DePamphilis, J. A. Ibers, and R. H. Holm, *J. Am. Chem. Soc.*, **97**, 1032 (1975).
(6) R. H. Holm and J. A. Ibers, in "Iron-Sulfur Proteins", Vol. III, W. Lovenberg, Ed., Academic Press, New York, N.Y., 1977, Chapter 7.
(7) R. H. Holm, *Acc. Chem. Res.*, **10**, 427 (1977).
(8) J. Cambray, R. W. Lane, A. G. Wedd, R. W. Johnson, and R. H. Holm, *Inorg. Chem.*, **16**, 2565 (1977).
(9) (a) M. A. Bobrik, K. O. Hodgson, and R. H. Holm, *Inorg. Chem.*, **16**, 1851 (1977); (b) G. B. Wong, M. A. Bobrik, and R. H. Holm, *Inorg. Chem.*, **17**, 578 (1977); (c) R. W. Johnson and R. H. Holm, *J. Am. Chem. Soc.*, in press.
(10) B. V. DePamphilis, B. A. Averill, T. Herskovitz, L. Que, Jr., and R. H. Holm, *J. Am. Chem. Soc.*, **96**, 4159 (1974).
(11) K. Mukai, J. J. Huang, and T. Kimura, *Biochim. Biophys. Acta*, **336**, 427 (1974).
(12) J. C. M. Tsibris, M. J. Namtvedt, and I. C. Gunsalus, *Biochem. Biophys. Res. Commun.*, **30**, 323 (1968).
(13) J. A. Fee and G. Palmer, *Biochim. Biophys. Acta*, **245**, 175 (1971).
(14) For examples of homologous S/Se complexes cf., e.g.: (a) R. H. Holm and M. J. O'Connor, *Prog. Inorg. Chem.*, **14**, 241 (1971); (b) K. A. Jensen and C. K. Jørgensen, in "Organic Selenium Compounds: Their Chemistry and Biology", D. L. Klayman and W. H. H. Günther, Ed., Wiley, New York, N.Y., 1973, Chapter XVI; (c) K. H. Schmidt and A. Müller, *Coord. Chem. Rev.*, **14**, 115 (1974).
(15) A. Davison and E. T. Shawl, *Inorg. Chem.*, **9**, 1820 (1970).
(16) Relevant reports include: (a) C. Furlani, E. Cervone, and F. D. Camassei, *Inorg. Chem.*, **7**, 265 (1968); (b) E. Cervone, F. D. Camassei, M. L. Luciani, and C. Furlani, *J. Inorg. Nucl. Chem.*, **31**, 1101 (1969); (c) K. A. Jensen, V. Krishnan, and C. K. Jørgensen, *Acta Chem. Scand.*, **24**, 743 (1970); (d) B. Lorenz, R. Kirmse, and E. Hoyer, *Z. Anorg. Allg. Chem.*, **378**, 144 (1970); (e) D. DeFilippo, P. Depalano, A. Diaz, S. Steffé, and E. T. Trogu, *J. Chem. Soc., Dalton Trans.*, 1566 (1977).
(17) (a) R. A. Schunn, C. J. Fritchie, Jr., and C. T. Prewitt, *Inorg. Chem.*, **5**, 892 (1966); (b) C.-H. Wei, R. G. Wilkes, P. M. Treichel, and L. F. Dahl, *ibid.*, **5**, 900 (1966).
(18) (a) Trinh-Toan, W. P. Fehlhammer, and L. F. Dahl, *J. Am. Chem. Soc.*, **99**, 402 (1977); (b) Trinh-Toan, B. K. Teo, J. A. Ferguson, T. J. Meyer, and L. F. Dahl, *ibid.*, **99**, 408 (1977).
(19) R. M. Roder, Ph.D. Thesis, University of Wisconsin–Madison, 1973; L. F. Dahl, private communication, June 1977.
(20) M. Laing, P. M. Kiernan, and W. P. Griffith, *Chem. Commun.*, 221 (1977).
(21) K. B. Sharpless and R. F. Lauer, *J. Am. Chem. Soc.*, **95**, 2697 (1973).
(22) D. L. Klayman and T. S. Griffin, *J. Am. Chem. Soc.*, **95**, 197 (1973).
(23) In addition to the local data reduction program ENXDR, the programs used included full-matrix least-squares and Fourier programs; ABSCOR, a numerical method absorption correction program which applies a Gaussian grid to the crystal; a modified version of ORFFE (Busing and Levy's function and error program); and Johnson's ORTEP. All calculations were carried out on a PDP 11/45 computer. Atomic scattering factors were taken from "International Tables for X-ray Crystallography", Vol. IV, Kynoch Press, Birmingham, England, 1974.
(24) Supplementary material.
(25) For an extensive list of references to structural determinations of cubane-like cluster compounds of the general type $M_4X_4L_{4n}$, cf. B.-K. Teo and J. C. Calabrese, *Inorg. Chem.*, **15**, 2467 (1976).
(26) The established cubane structure of $[Re_4(SMe)_4(CO)_{12}]$[27] suggests that the species $[M(SeR)(CO)_3]_n$ (M = Mn, Re)[28] may have similar structures with triply bridging RSe ligands. The above species appear to be the only previously known $M_4X_4L_{4n}$ cases in which X is unsubstituted selenide.
(27) W. Harrison, W. C. Marsh, and J. Trotter, *J. Chem. Soc., Dalton Trans.*, 1009 (1972).
(28) E. W. Abel, B. C. Crosse, and G. V. Hutson, *J. Chem. Soc. A*, 2014 (1967).
(29) C. J. Fritchie, Jr., *Acta Crystallogr., Sect. B*, **31**, 802 (1975).
(30) Note that division of Fe–Fe distances in Table III such that the longer and shorter values are associated with faces approximately parallel and perpendicular, respectively, to the $\bar{4}$ axis is somewhat arbitrary. An equally valid division is: 2 long (Fe(1)–Fe(4), Fe(2)–Fe(3)) + 4 short (Fe(1)–Fe(2), –Fe(3); Fe(4)–Fe(2), –Fe(3)).
(31) M. Bonamico and G. Dessy, *J. Chem. Soc. A*, 264 (1971).
(32) P. T. Beurskens and J. A. Cras, *J. Cryst. Mol. Struct.*, **1**, 63 (1971); J. P. Fackler, Jr., A. Avdeef, and R. G. Fischer, Jr., *J. Am. Chem. Soc.*, **95**, 774 (1973).
(33) A. E. Smith, G. N. Schrauzer, V. P. Mayweg, and W. Heinrich, *J. Am. Chem. Soc.*, **87**, 5798 (1965); C. G. Pierpont and R. Eisenberg, *J. Chem. Soc. A*, 2285 (1971).
(34) P. Goldstein and A. Paton, *Acta Crystallogr., Sect. B*, **30**, 915 (1974).
(35) C. H. Wei and L. F. Dahl, *Inorg. Chem.*, **4**, 493 (1965); L. F. Dahl and P. W. Sutton, *ibid.*, **2**, 1067 (1963).
(36) V. Schomaker and D. P. Stevenson, *J. Am. Chem. Soc.*, **63**, 37 (1941).
(37) C. Y. Yang, K. H. Johnson, R. H. Holm, and J. G. Norman, Jr., *J. Am. Chem. Soc.*, **97**, 6596 (1975).
(38) C. K. Jørgensen, *Inorg. Chim. Acta, Rev.*, **2**, 65 (1968).
(39) A. Müller, E. Diemann, and C. K. Jørgensen, *Struct. Bonding (Berlin)*, **14**, 23 (1973).
(40) R. Heber, R. Kirmse, and E. Hoyer, *Z. Anorg. Allg. Chem.*, **393**, 159 (1972).
(41) H. H. Schmidtke, *Ber. Bunsenges. Phys. Chem.*, **71**, 1138 (1967).
(42) C. K. Jørgensen, *Prog. Inorg. Chem.*, **12**, 101 (1970).
(43) J. A. Ferguson and T. J. Meyer, *Chem. Commun.*, 623 (1971).
(44) Like salts of $[Fe_4S_4(SPh)_4]^{2-}$[45] this compound showed substantial paramagnetic impurity as evidenced by a minimum in the susceptibility vs. temperature plot at 65 K. An impurity correction was made by fitting the data to an equation of the form $\chi_{impurity} = C/T$ for $T \leq T_{min}$ and taking the intercept (525×10^{-6} cgsu/tetramer) as an apparent temperature-independent paramagnetism. Magnetic moments were calculated from $\mu_t = 2.829(\chi_t^{cor}T)^{1/2}$.
(45) E. J. Laskowski, R. B. Frankel, W. O. Gillum, G. C. Papaefthymiou, J. Renaud, J. A. Ibers, and R. H. Holm, *J. Am. Chem. Soc.*, in press.
(46) R. Cammack, *Biochem. Soc. Trans.*, **3**, 482 (1975); *J. Phys. (Paris)*, **38** C6-137 (1976).
(47) (a) T. C. Stadtman, *Science*, **183**, 915 (1974); (b) D. V. Frost and P. M. Lish, *Annu. Rev. Pharmacol.*, **15**, 259 (1975).

(48) W. G. Hoekstra, *Fed. Proc., Fed. Am. Soc. Exp. Biol.*, **34**, 2083 (1975).
(49) J. R. Andreesen and L. G. Ljungdahl, *J. Bacteriol.*, **116**, 867 (1973); **120**, 6 (1974).
(50) J. E. Cone, R. Martin del Río, J. N. Davis, and T. C. Stadtman, *Proc. Natl. Acad. Sci. U.S.A.*, **73**, 2659 (1976).
(51) A. T. Diplock and J. A. Lucy, *FEBS Lett.*, **29**, 205 (1973); A. S. M. Giasuddin, C. P. J. Caygill, A. T. Diplock, and E. H. Jeffery, *Biochem. J.*, **146**, 339 (1975).
(52) I. C. Gunsalus, J. R. Meeks, J. D. Lipscomb, P. Debrunner, and E. Münck in "Molecular Mechanisms of Oxygen Activation", O. Hayaishi, Ed., Academic Press, New York, N.Y., 1973, Chapter 14. For probable identification of one such protein from liver microsomal fractions as a 2-Fe ferredoxin, cf. J. I. Pedersen, H. Oftebro, and T. Vänngård, *Biochem. Biophys. Res. Commun.*, **76**, 666 (1977).
(53) J. A. Fee, S. G. Mayhew, and G. Palmer, *Biochim. Biophys. Acta*, **245**, 196 (1971).
(54) G. S. Wilson, J. C. M. Tsibris, and I. C. Gunsalus, *J. Biol. Chem.*, **248**, 6059 (1973).
(55) Y. Sugiura, K. Ishizu, T. Kimura, and H. Tanaka, *Bioinorg. Chem.*, **4**, 291 (1975).

Contribution from the Department of Chemistry, Bateman Science Center, Arizona State University, Tempe, Arizona 85281

Synthesis, Characterization, and Molecular Structure of Sulfidotris(*N*,*N*-diethyldithiocarbamato)tantalum(V)

E. J. PETERSON, R. B. VON DREELE,* and T. M. BROWN*

Received August 12, 1977

The synthesis of the title compound has been accomplished and classical physical methods have been employed to characterize the complex. The crystal and molecular structures have also been determined from single-crystal x-ray intensity data collected by the θ–2θ scan technique. The molecule is monomeric with seven sulfur atoms bound to the Ta(V) atom at the corners of a distorted pentagonal bipyramid. The monodentate sulfur atom, doubly bonded to the tantalum atom, occupies one axial position (Ta–S = 2.181 (1) Å), one diethyldithiocarbamate ligand spans the other axial position and one equatorial position, and two diethyldithiocarbamate ligands occupy the remaining equatorial positions. The bond distance between the tantalum and the axial sulfur atom opposite Ta=S is ca. 0.13 Å longer than the average length of the five equatorial bonds (Ta–S_{eq} = 2.556 Å). Because of the extremely close S···S contacts in the equatorial plane, the pentagonal girdle of sulfur atoms is appreciably puckered. The observed distortions from the ideal pentagonal-bipyramidal geometry are considered in relation to steric effects. The structure was solved by standard heavy-atom techniques and refined by full-matrix least squares to a final *R* value of 0.037 for 5055 independent observed reflections. The compound crystallized in the monoclinic space group $P2_1/c$, $Z = 4$, and has lattice parameters $a = 9.647$ (4) Å, $b = 17.214$ (7) Å, $c = 15.442$ (6) Å, and $\beta = 96.78$ (3)° ($\rho_{calcd} = 1.704$ g cm^{-3}; $\rho_{obsd} = 1.703$ g cm^{-3}).

Introduction

Tantalum, as well as the other early transition metals, exhibits a marked preference for higher coordination numbers, and coordination number seven for it has recently been established by x-ray diffraction studies. A tetragonal face capped trigonal prism geometry, with a chloride as the capping ligand, has been used to describe the coordination polyhedron in $Me_3TaCl_2(bpy)$.[1] Orthorhombic and monoclinic forms of the acetamidinates $TaCl_3(C_6H_{11}N{=}C(Me)NC_6H_{11})_2$ and $TaCl_3(C_6H_{11}N{=}C(Me)NC_6H_{11})(C_6H_{11}NC(NHC_6H_{11}){=}O)$ have recently been found to adopt this same geometry.[2-5] However, another acetamidinate complex, $MeTaCl_2(C_6H_{11}N{=}C(Me)NC_6H_{11})_2$, has the two bidentate ligands mutually perpendicular, and the molecular geometry could not be related to any idealized polyhedron.[6] In contrast, the diarsine complex of tantalum(V) originally formulated[7] as a seven-coordinate complex, $TaBr_5(diars)$, has recently been found by x-ray diffraction[8] to be $[TaBr_4(diars)_2]^+[TaBr_6]^-$.

Sulfidotris(*N*,*N*-diethyldithiocarbamato)tantalum(V), $TaS(S_2CNEt_2)_3$, was first reported by Heckley et al.[9] These authors isolated a green crystalline compound which they analyzed by classical characterization techniques to be a seven-coordinate complex. The work described in this paper was undertaken when a yellow compound was isolated from a different preparation and was also formulated as $TaS(S_2CNEt_2)_3$. The yellow crystalline compound was examined by the single-crystal x-ray diffraction technique, as well as by classical methods, in order to unequivocally confirm the coordination number and the establish the geometry of the coordination polyhedron.

Experimental Section

Due to the sensitivity of starting materials to hydrolysis, it was necessary to rigorously exclude water during preparation, handling, and storage. In order to maintain these conditions, standard inert-atmosphere and vacuum techniques were employed. The reaction–extraction vessel used in the preparation was described previously.[10] The vessel was evacuated and heated prior to use to remove residual traces of water.

Materials. Tantalum(V) chloride obtained from Research Inorganic Chemicals was purified by sublimation. Sodium diethyldithiocarbamate trihydrate was obtained from Aldrich Chemical Co., washed with three 50-mL portions of hot diethyl ether, and dried at 60 °C in vacuo before use. Analytical reagent grade acetonitrile, obtained from Mallinckrodt Chemical Works, was dried and outgassed over phosphorus pentoxide and stored over Linde type 4A molecular sieves. Immediately prior to use, the acetonitrile was vacuum distilled onto CaH_2 and again outgassed in order to ensure anhydrous conditions.

Preparation and Characterization of $TaS(S_2CNEt_2)_3$. In a typical preparation, 2 g of $TaCl_5$ (0.0056 mol) and 4.77 g of sodium diethyldithiocarbamate (0.0279 mol) were placed in one end of the reaction–extraction vessel. Approximately 60 mL of acetonitrile was vacuum distilled onto the reactants, and stirring was initiated and continued for a period of 3 h at ambient temperature. The vessel was then inverted and the brown solution was filtered away from the insoluble NaCl. This solution was allowed to stand undisturbed in vacuo for a period of several weeks. During this time, a yellow crystalline compound separated from the acetonitrile solution (which remained brown) and was isolated by filtration. The formation of the yellow compound could be accelerated by heating the acetonitrile solution to reflux. The yellow crystals appeared to resist hydrolysis indefinitely. Anal. Calcd for $TaS_7C_{15}N_3H_{30}$: C, 27.41; H, 4.57; N, 6.40; S, 34.09. Found: C, 27.44; H, 4.47; N, 6.33; S, 33.61. NMR (CD_3CN solution, 35 °C): 1.20 ppm (triplet, CH_3) and 3.70 ppm (quartet, CH_2) relative to an internal reference of tetramethylsilane. IR (Nujol mull): ν(C=N) 1520 cm^{-1}, $\nu(NC_2)$ 1155 cm^{-1}, ν(C=S) 1010 cm^{-1}, ν(Ta=S) 905 cm^{-1}, ν(Ta–S) 360 cm^{-1} (all assigned bands were strong and sharp).

Crystal Data and Data Collection. Because of the apparent insensitivity of the crystals to moisture, a suitable crystal of approximate dimensions 0.3 × 0.3 × 0.2 mm was mounted in a random orientation on the end of a glass fiber. On the basis of precession photographs, the lattice was assigned to the monoclinic system. The systematic absences of $0k0$ for k odd and $h0l$ for l odd are consistent with the centrosymmetric space group $P2_1/c$ (C_{2h}^5).[11] There were 57 strong

0020-1669/78/1317-1410$01.00/0